Macromolecules **2004,** *37,* 7938−7944

Solid-State Polymerizations of 7-Alkoxycarbonyl-7-cyano-1,4-benzoquinone Methides

Takahito Itoh,*,† Shinji Nomura,† Nagisa Saitoh,† Takahiro Uno,† Masataka Kubo,† Kazuki Sada,‡ Katsunari Inoue,§ and Mikiji Miyata§

Department of Chemistry for Materials, Faculty of Engineering, Mie University, 1515 Kamihama-cho,
Tsu-shi, Mie 514-8507, Japan; Department of Chemistry and Biochemistry,
Graduate School of Engineering, Kyushu University, 6-10-1 Hakozaki, Higashi-ku,
Fukuoka 630-8528, Japan; and Department of Material and Life Science,
Graduate School of Engineering, Osaka University and Handai FRC, 2-1 Yamadaoka,
Suita, Osaka 565-0871, Japan

Received March 1, 2004; Revised Manuscript Received July 28, 2004

ABSTRACT: Thermal polymerizations and photopolymerizations of 7-alkoxycarbonyl-7-cyano-1,4-benzoquinone methides (methoxy (**2a**), ethoxy (**2b**), propoxy (**2c**), isopropoxy (**2d**), butoxy (**2e**), and *sec*-butoxy (**2f**)) were investigated in the solid state. In the thermal polymerization in the solid state, **2a, 2c**, **2d**, and **2e** polymerized to give glassy solids or a mass of crystals, but both **2b** and **2f** did not polymerize. In the photopolymerization in the solid state, all monomer crystals except for **2a** polymerized to give corresponding polymers as needlelike solids. The needlelike polymer obtained by photopolymerization of highly reactive **2c** was amorphous by powder X-ray diffraction measurement. Crystal structure of **2c** was determined by single-crystal X-ray structure analysis, and the molecular packing in the crystals was discussed.

Introduction

Solid-state polymerization implies that polymerization proceeds starting from bulk monomer crystals, and it has been divided into two classes: topotactic and topochemical polymerizations.[1] The former is the polymerization that provides a polymer with a specific crystal structure formed under control of the crystal lattice of the monomer, and the latter is the polymerization that proceeds with no movement of the center of gravity of the monomer molecule and only slight rotation of the monomer molecule around the gravity; that is, the crystallographic position and symmetry of the monomer crystals are retained in the resulting polymer crystals. Therefore, topochemical polymerization is a promising method to obtain polymers with highly controlled structures. A limited number of monomers such as derivatives of diacetylene,[1] 2,5-distyrylpyrazine,[2] triene and triacetylene,[3] and muconic acid and sorbic acid[4] have been reported to undergo topochemical polymerizations. Recently, we reported that 7,7,8,8-tetrakis(methoxycarbonyl)quinodimethane (**1a**) gave two crystal forms, and they exhibited drastic differences in the polymerization ability between them and also polymerization proceeds topochemically.[5] Moreover, we synthesized novel 7,7,8,8-tetrakis(alkoxycarbonyl)quinodimethanes (**1b**−**f**) with various alkoxy groups and discussed the relationship of the solid-state polymerization reactivity with the molecular packing in the crystals on the basis of crystal structure analysis.[6] As the result, we found principles for the topochemical polymerizations of quinodimethane monomers in the solid state to predict the polymerization reactivity. In the crystals of the polymerizable monomers, monomer molecules stack in a columnar structure with the angle formed between the stacking axis and longer axis of quinodimethane moiety of 30−33° and the distance between equivalent atoms in the stacked monomers of 7.0−7.6 Å.[6] Quinone methides are a member of quinoid family; it was reported that they are isolable as crystal forms at room temperature, and their polymerization behavior in solution is similar to that of the substituted quinodimethanes in solution.[7−10] If they have molecular stacking mode in the crystals similar to the quinodimethanes **1a**−**f**, they are expected to polymerize topochemically. To expand the scope of monomers that undergo polymerization topochemically, we investigated the solid-state polymerization reactivities of a series of 7-alkoxycarbonyl-7-cyano-1,4-benzoquinone methides (methoxy (**2a**), ethoxy (**2b**), propoxy (**2c**), isopropoxy (**2d**), butoxy (**2e**), and *sec*-butoxy (**1f**)).

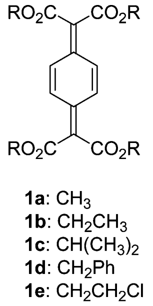

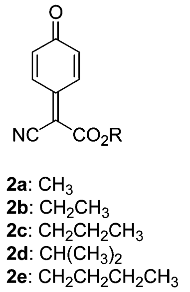

Experimental Section

Measurements. All melting points were obtained with a Yanaco MP-50 melting point apparatus. The number-average molecular weights, M_n, of the polymers were determined by gel permeation chromatography (GPC) on a Jasco PU-2080 Plus equipped with TOSOH UV-8020 ultraviolet (254 nm) detector and TSK gel G2500H$_8$ (bead size with 10 μm, molecular weight range 1.0×10^2−2.0×10^4) and TSK gel

---

† Mie University.

‡ Kyushu University.

§ Osaka University and Handai FRC.

* Corresponding author: phone +81-59-231-9410; Fax +81-59-231-9410; e-mail itoh@chem.mie-u.ac.jp.

10.1021/ma049596r CCC: $27.50

Scheme 1

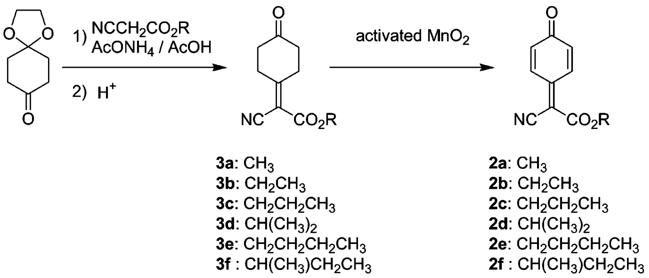

G3000H$_8$ (bead size with 10 μm, molecular weight range 1.0 $\times$ 10^2−6.0 $\times$ 10^4) using tetrahydrofuran (THF) as an eluent at a flow rate of 1.0 mL/min and polystyrene standards for calibration. The NMR and IR spectra were recorded on a JEOL JNM-EX270 FT NMR spectrometer using chloroform-*d* with tetramethylsilane as an internal standard at 25 °C and a JASCO IR-700 spectrometer, respectively.

The powder X-ray diffraction (XRD) measurement of the polymers was carried out using a Rigaku Rotaflex RU-200B in the 2θ range from 10° to 90° at a scan speed of 0.5°/min with sampling width of 0.02°. The graphite-monochromated Cu Kα line (λ = 1.541 78 Å) was used with the power of the X-ray generator 40 kV and 150 mA. The single-crystal X-ray data were collected on a Rigaku RAXIS-RAPID imaging plate diffractometer using Cu Kα radiation (λ = 1.541 78 Å) monochromated with graphite. The structure was solved by the direct methods with the program SIR88 and refined by full-matrix least-squares procedures. The calculation was performed using the TEXSAN crystallographic software package of the Molecular Structure Corp.

Monomer Synthesis. 4-[(Alkoxycarbonyl)cyanomethylene]-cyclohexanones (**3a**−**f**) and 7-alkoxycarbonyl-7-cyano-1,4-benzoquinone methides (**2a**−**f**), including new compounds **2c** and **3c**, were synthesized by the same procedure reported previously (Scheme 1).[7,8]

4-[(Alkoxycarbonyl)cyanomethylene]cyclohexanones (3a−f). General Preparation Method. 1,4-Cyclohexanedione monoethylene ketal (10 g, 64 mmol) and alkyl cyanoacetate (70 mmol) were refluxed in the presence of 0.4 g of ammonium acetate and 2 mL of acetic acid in 150 mL of toluene using a Dean−Stark water separator to isolate water formed for 48 h. The reaction mixture was washed twice with 100 mL of water and dried over anhydrous magnesium sulfate. It was placed under reduced pressure to remove toluene to give a pale yellow solid, to which was added 200 mL of a 2% aqueous sulfuric acid solution, and refluxed for 1 h. After cooling, the reaction mixture was extracted with chloroform (400 mL $\times$ 3). The combined organic fractions were washed twice with 100 mL of water, dried over anhydrous magnesium sulfate, and filtered, and the solvent of the filtrate was evaporated under reduced pressure. The crude product was purified by column chromatography (SiO$_2$, chloroform) followed by recrystallization from hexane.

4-[Cyano(methoxycarbonyl)methylene]cyclohexanone (3a). From dimethyl malonate, **3a** was obtained as white needles (69% yield); mp 67−69 °C. IR (KBr, cm^{-1}): ν_{CN} 2200, $\nu_{C=O}$ 1686, $\nu_{C=C}$ 1568, ν_{C-O} 1238, 1095. ^{1}H NMR (CDCl$_3$): δ 3.86 (s, 3H), 3.42 (t, J = 6.9 Hz, 2H), 3.14 (t, J = 6.9 Hz, 2H), 2.56 (m, 4H). ^{13}C NMR (CDCl$_3$): δ 208.3, 175.0, 161.6, 114.6, 104.2, 52.6, 36.8, 36.7, 31.8, 27.9. Anal. Calcd for C$_{10}$H$_{11}$NO$_3$: C, 62.16%; H, 5.74%; N, 7.25%. Found: C, 61.85%; H, 5.73%; N, 7.32%.

4-[Cyano(ethoxycarbonyl)methylene]cyclohexanone (3b). From diethyl malonate, **3b** was obtained as white needles (55% yield); mp 57−59 °C. IR (KBr, cm^{-1}): ν_{CN} 2202, $\nu_{C=O}$ 1692, $\nu_{C=C}$ 1565, ν_{C-O} 1236, 1087. ^{1}H NMR (CDCl$_3$): δ 4.29 (q, J = 7.2 Hz, 2H), 3.40 (t, J = 6.9 Hz, 2H), 3.13 (t, J = 6.9 Hz, 2H), 2.55 (m, 4H), 1.37 (t, J = 7.2 Hz, 3H). ^{13}C NMR (CDCl$_3$): δ 208.6, 174.6, 161.7, 115.1, 105.2, 62.4, 37.3, 37.2, 32.2, 28.3, 14.4. Anal. Calcd for C$_{11}$H$_{13}$NO$_3$: C, 63.75%; H, 6.32%; N, 6.76%. Found: C, 63.90%; H, 6.58%; N, 6.67%.

4-[Cyano(propoxycarbonyl)methylene]cyclohexanone (3c). From dipropyl malonate, **3c** was obtained as white needles (70% yield); mp 87−88 °C. IR (KBr, cm^{-1}): ν_{CN} 2198, $\nu_{C=O}$ 1687, $\nu_{C=C}$ 1563, ν_{C-O} 1235, 1101. ^{1}H NMR (CDCl$_3$): δ 4.20 (q, J = 6.6 Hz, 2H), 3.41 (t, J = 6.9 Hz, 2H), 3.13 (t, J = 6.9 Hz, 2H), 2.55 (m, 4H), 1.74 (m, 2H), 1.01 (t, J = 7.6 Hz, 3H). ^{13}C NMR (CDCl$_3$): δ 208.2, 174.2, 161.3, 114.6, 104.7, 67.4, 33.9, 36.8, 31.8, 27.9, 21.7, 10.2. Anal. Calcd for C$_{12}$H$_{15}$NO$_3$: C, 65.14%; H, 6.83%; N, 6.33%. Found: C, 64.98%; H, 6.89%; N, 6.35%.

4-[Cyano(isopropoxycarbonel)methylene]cyclohexanone (3d). From diisopropyl malonate, **3d** was obtained as white needles (80% yield); mp 52−54 °C. IR (KBr cm^{-1}): ν_{CN} 2198, $\nu_{C=O}$ 1670, $\nu_{C=C}$ 1566, ν_{C-O} 1233, 1086. ^{1}H NMR (CDCl$_3$): δ 5.12 (m, J = 6.3 Hz, 2H), 3.40 (t, J = 6.9 Hz, 2H), 3.12 (t, J = 6.9 Hz, 2H), 2.54 (m, 4H), 1.33 (d, J = 6.3 Hz, 6H). ^{13}C NMR (CDCl$_3$): δ 208.3, 173.7, 160.8, 114.7, 105.2, 70.0, 37.0, 36.9, 31.8, 27.9, 21.5. Anal. Calcd for C$_{12}$H$_{15}$NO$_3$: C, 65.14%; H, 6.83%; N, 6.33%. Found: C, 65.14%; H, 6.91%; N, 6.32%.

4-[Cyano(butoxycarbonyl)methylene]cyclohexanone (3e). From dibutyl malonate, **3e** was obtained as white needles (85% yield); mp 65−66 °C. IR (KBr, cm^{-1}): ν_{CN} 2198, $\nu_{C=O}$ 1684, $\nu_{C=C}$ 1564, ν_{C-O} 1192, 1094. ^{1}H NMR (CDCl$_3$): δ 4.25 (t, J = 6.6 Hz, 2H), 3.40 (t, J = 6.9 Hz, 2H), 3.13 (t, J = 6.9 Hz, 2H), 2.55 (m, 4H), 1.71 (m, 2H), 1.43 (m, 2H), 0.96 (t, J = 7.4 Hz, 3H). ^{13}C NMR (CDCl$_3$): δ 208.2, 174.1, 161.3, 114.6, 104.8, 65.8, 36.95, 36.86, 31.8, 30.3, 27.9, 18.9, 13.5. Anal. Calcd for C$_{13}$H$_{17}$NO$_3$: C, 66.36%; H, 7.29%; N, 5.95%. Found: C, 66.21%; H, 7.37%; N, 5.99%.

4-[Cyano(*sec*-butoxycarbonyl)methylene]cyclohexanone (3f). From di(*sec*-butyl) malonate, **3f** was obtained as a yellow oil (85% yield). IR (neat, cm^{-1}): ν_{CN} 2204, $\nu_{C=O}$ 1681, $\nu_{C=C}$ 1572, ν_{C-O} 1234, 1084. ^{1}H NMR (CDCl$_3$): δ 4.94 (m, 1H), 3.41 (t, J = 6.9 Hz, 2H), 3.13 (t, J = 6.9 Hz, 2H), 2.58 (m, 4H), 1.67 (m, 2H)1.30 (d, J = 6.3 Hz, 3H), 0.95 (t, J = 7.6 Hz, 3H). ^{13}C NMR (CDCl$_3$): δ 208.3, 173.7, 160.9, 114.7, 105.2, 74.5, 36.95, 36.86, 31.8, 28.5, 27.9, 19.2, 9.4. Anal. Calcd for C$_{13}$H$_{17}$NO$_3$: C, 66.36%; H, 7.29%; N, 5.95%. Found: C, 66.39%; H, 7.35%; N, 5.92%.

7-Alkoxycarbonyl-7-cyano-1,4-benzoquinone Methides (2a−f). **General Preparation Method.** About 2 g of **3a**−**f** was dissolved in 800 mL of chloroform, and then into the resulting solution were added 10 g of activated manganese dioxide and 10 g of 3 Å molecular sieves. The mixture was refluxed with stirring for 40 min, cooled, and then filtered. The orange filtrate was placed under reduced pressure to remove chloroform to give an orange solid residue, which was dissolved in a small amount of chloroform. The resulting solution was passed through a silica gel column by using chloroform as an eluent. The orange elution band was collected and placed under reduced pressure to remove solvent to obtain an orange solid, which was recrystallized from hexane to give orange needles.

7-Cyano-7-(methoxycarbonyl)-1,4-benzoquinone Methide (2a). Yield 26%; mp 105−108 °C. IR (KBr, cm^{-1}): ν_{CN} 2194, $\nu_{C=O}$ 1699, $\nu_{C=C}$ 1608, ν_{C-O} 1222, 1068. ^{1}H NMR (CDCl$_3$): δ 8.60 (d, J = 10.2 Hz, 1H), 7.70 (d, J = 10.2 Hz, 1H), 6.64 (d, J = 10.2 Hz, 1H), 6.56 (d, J = 10.2 Hz, 1H), 3.97 (s, 3H). ^{13}C NMR (CDCl$_3$): δ 186.1, 160.9, 148.8, 136.1, 133.5, 132.7, 132.5, 114.5, 111.2, 53.8. UV (CHCl$_3$) λ 320 nm (ϵ = 3.18 $\times$ 10^4). Anal. Calcd for C$_{10}$H$_7$NO$_3$: C, 63.49%; H, 3.73%; N, 7.40%. Found: C, 62.38%; H, 3.56%; N, 7.73%.

7-Cyano-7-(ethoxycarbonyl)-1,4-benzoquinone Methide (2b). Yield 20%; mp 57−59 °C. IR (KBr, cm^{-1}): ν_{CN} 2194, $\nu_{C=O}$ 1704, $\nu_{C=C}$ 1611, ν_{C-O} 1223. ^{1}H NMR (CDCl$_3$): δ 8.56 (d, J = 10.2 Hz, 1H), 7.71 (d, J = 10.2 Hz, 1H), 6.63 (d, J = 10.2 Hz, 1H), 6.56 (d, J = 10.2 Hz, 1H), 4.40 (q, J = 7.2 Hz, 2H), 1.42 (t, J = 7.2 Hz, 3H). ^{13}C NMR (CDCl$_3$): δ 186.1, 160.9, 148.4, 136.2, 133.4, 132.8, 132.3, 114.4, 111.4, 63.4, 13.89. UV (CHCl$_3$) λ 320 nm (ϵ = 3.08 $\times$ 10^4). Anal. Calcd for C$_{11}$H$_9$NO$_3$: C, 65.02%; H, 4.46%; N, 6.89%. Found: C, 64.81%; H, 4.43%; N, 6.95%.

7-Cyano-7-(propoxycarbonyl)-1,4-benzoquinone Methide (2c). Yield 22%; mp 68−69.5 °C. IR (KBr, cm^{-1}): ν_{CN}

Table 1. Thermal Polymerizations of 2a−f in the Solid State

run	monomer	mp, °C	temp, °C	time, h	form	conv, %	$M_n/10^4$	M_w/M_n
1	**2a** (Me)	105	95	24	melt	51	0.4	1.77
2	**2b** (Et)	57	50	24	needle	0		
3	**2c** (Pr)	68	60	48	mass	10	3.8	1.51
4	**2d** (^{i}Pr)	91	80	24	mass	81	2.1	1.45
5	**2e** (Bu)	61	50	48	mass	41	3.1	1.52
6	**2f** (^{s}Bu)	58	50	48	needle	0	-	

2194, $\nu_{C=O}$ 1699, $\nu_{C=C}$ 1608, ν_{C-O} 1222, 1068. ^{1}H NMR ($CDCl_3$): δ 8.59 (d, J = 10.2 Hz, 1H), 7.71 (d, J = 10.2 Hz, 1H), 6.63 (d, J = 10.2 Hz, 1H), 6.56 (d, J = 10.2 Hz, 1H), 4.31 (t, J = 6.6 Hz, 2H), 1.79 (m, 2H), 1.04 (t, J = 7.6 Hz, 3H). ^{13}C NMR ($CDCl_3$): δ 186.1, 160.5, 148.4, 136.2, 132.8, 114.4, 111.4, 68.8, 21.7, 10.2. UV ($CHCl_3$) λ 304 nm ($\epsilon = 3.15 \times 10^4$). Anal. Calcd for $C_{12}H_{11}NO_3$: C, 66.35%; H, 5.10%; N, 6.45%. Found: C, 65.54%; H, 4.97%; N, 6.37%.

7-Cyano-7-(isoproxycarbonyl)-1,4-benzoquinone Methide (2d). Yield 25%; mp 91−92 °C. IR (KBr, cm^{-1}): ν_{CN} 2196, $\nu_{C=O}$ 1687, $\nu_{C=C}$ 1540, ν_{C-O} 1250, 1087. ^{1}H NMR ($CDCl_3$): δ 8.58 (d, J = 10.2 Hz, 1H), 7.69 (d, J = 10.2 Hz, 1H), 6.59 (d, J = 10.2 Hz, 1H), 6.52 (d, J = 10.2 Hz, 1H), 5.22 (m, J = 6.3 Hz, 1H), 1.41 (d, J = 6.3 Hz, 6H).^{13}C NMR ($CDCl_3$): δ 186.1, 160.0, 148.2, 136.3, 133.4, 132.9, 132.3, 114.5, 111.9, 71.93, 21.57. UV ($CHCl_3$) λ 321 nm ($\epsilon = 3.18 \times 10^4$). Anal. Calcd for $C_{12}H_{11}NO_3$: C, 66.35%; H, 5.10%; N, 6.45%. Found: C, 66.35%; H, 5.01%; N, 6.47%.

7-Cyano-7-(butoxycarbonyl)-1,4-benzoquinone Methide (2e). Yield 22%; mp 61−62 °C. IR (KBr): ν_{CN} 2196, $\nu_{C=O}$ 1680, $\nu_{C=C}$ 1610, ν_{C-O} 1247, 1069. ^{1}H NMR ($CDCl_3$): δ 8.55 (d, J = 10.2 Hz, 1H), 7.73 (d, J = 10.2 Hz, 1H), 6.63 (d, J = 10.2 Hz, 1H), 6.52 (d, J = 10.2 Hz, 1H), 4.35 (t, J = 6.6 Hz, 2H), 1.76 (m, 2H), 1.54 (m, 2H), 0.98 (t, J = 7.3 Hz, 3H). ^{13}C NMR ($CDCl_3$): δ 186.3, 160.6, 148.5, 136.2, 133.4, 132.8, 132.4, 114.48, 111.7, 67.2, 30.3, 19.0, 13.6. UV ($CHCl_3$) λ 320 nm ($\epsilon = 3.26 \times 10^4$). Anal. Calcd for $C_{13}H_{13}NO_3$: C, 67.52%; H, 5.67%; N, 6.06%. Found: C, 67.40%; H, 5.61%; N, 6.10%.

7-Cyano-7-(*sec*-butoxycarbonyl)-1,4-benzoquinone Methide (2f). Yield 11%; mp 57.5−58 °C. IR (KBr, cm^{-1}): ν_{CN} 2192, $\nu_{C=O}$ 1682, $\nu_{C=C}$ 1587, ν_{C-O} 1233, 1097. ^{1}H NMR ($CDCl_3$): δ 8.55 (d, J = 10.2 Hz, 1H), 7.70 (d, J = 10.2 Hz, 1H), 6.59 (d, J = 10.2 Hz, 1H), 6.55 (d, J = 10.2 Hz, 1H), 5.04 (m, 1H), 1.74 (m, 2H), 1.38 (d, J = 6.3 Hz, 3H), 0.98 (t, J = 7.6 Hz, 3H). ^{13}C NMR ($CDCl_3$): δ 186.1, 160.1, 148.2, 136.2, 133.3, 132.9, 132.3, 114.4, 112.1, 76.4, 28.5, 19.2, 9.4. UV ($CHCl_3$) λ 320 nm ($\epsilon = 3.06 \times 10^4$). Anal. Calcd for $C_{13}H_{13}NO_3$: C, 67.52%; H, 5.67%; N, 6.06%. Found: C, 67.37%; H, 5.65%; N, 6.09%.

Polymerization Procedures. For solid-state polymerizations, a given amount of monomer crystal was put into a Pyrex ampule, which was degassed under reduced pressure and then sealed. Thermal polymerization was carried out by setting the ampule in an oil bath at a temperature 10 °C lower than each melting point of monomers **2a**−**f** for a given time. Photopolymerization was carried out at 30−35 °C under UV irradiation by using a high-pressure mercury lamp (Fuji Glass Work Type BH-400, 400 W) at a distance of 12 cm. The conversion was determined from the ratio of the peak area due to quinoid protons of **2a**−**f** to that due to the phenylene protons of polymer by ^{1}H NMR spectroscopy.

Results and Discussions

Solid-State Polymerization. Previously, we reported that 7,7,8,8-tetrakis(alkoxycarbonyl)quinodimethanes gave two crystal forms depending upon the recrystallization conditions, which have different polymerization reactivity in the solid state.[5,6] Unfortunately, all monomers **2a**−**f** gave only one crystal form under all attempted recrystallization conditions. Here, orange needles obtained by the recrystallization from hexane were used for the solid-state polymerizations.

Table 2. Photopolymerizations of 2a−f in the Solid State

run	monomer	time, h	form	conv, %	$M_n/10^4$	M_w/M_n
1	**2a** (Me)	70	needle solid	0		
2	**2b** (Et)	70	needlelike solid	69	1.6	1.56
3	**2c** (Pr)	70	needlelike solid	100	1.4	1.45
4	**2d** (^{i}Pr)	70	needlelike solid	100	1.0	1.47
5	**2e** (Bu)	70	needlelike solid	47	2.1	1.49
6	**2f** (^{s}Bu)	70	needlelike solid	18	1.6	1.67

We tried thermal polymerizations of these monomer crystals **2a**−**f** by heating in dark at a temperature 10 °C lower than each melting point, and the results are summarized in Table 1.

2a, **2c**, **2d**, and **2e** polymerized to give the corresponding polymers as glassy solids or a mass of crystals, which were soluble in chloroform, THF, benzene, and dichloromethane but insoluble in hexane, methanol, and diisopropyl ether. With the progress of polymerization, monomer needle crystals of **2a** gradually melted to form glassy solids, and monomer needle crystals of **2c**, **2d**, and **2e** each became a mass of crystals without melting, indicating that the collapse of the crystals takes place during polymerization. The number-average molecular weights (M_n) of obtained polymers were determined to be 4000−38 000 by GPC. No polymerizations occurred for **2b** and **2f**, and unreacted monomers were recovered quantitatively. The change by appearance of these monomer crystals in the thermal polymerizations indicates that all monomers **2b**−**f** do not polymerize with retaining crystal lattice.

Next, we tried polymerizations of these monomer crystals **2a**−**f** by irradiation using a 400 W high-pressure Hg lamp at 30−35 °C, and the results are shown in Table 2.

Shapes of the monomer needle crystals did not change during irradiation, but their orange color changed to pale yellow for **2b**−**f** and was retained for **2a**. The monomers **2b**−**f** polymerized to give corresponding polymers with the M_n of 10 000−21 000, but **2a** did not polymerize. As the monomer crystals of **2b**−**f** did not polymerize in the dark at 30−35 °C, polymer formation upon UV irradiation is due to photoinitiation. In this photopolymerization, both **2c** and **2d** showed the highest polymerization reactivity among the monomers **2a**−**f**, and the **2a** and **2b** with less bulky substituents (methoxy and ethoxy groups) and the **2e** and **2f** with bulky substituents (butoxy and *tert*-butoxy groups) were less reactive. The relationship of the polymerization reactivity with substituents for the quinoid monomers such as 7-alkoxycarbonyl-7-cyano-1,4-benzoquinone methides,[7,8] 7,7-bis(alkoxycarbonyl)-1,4- benzoquinone methides,[9] 7,8-diacyl-7,8-dicyanoquinodimethanes,[11−13] 7,8-bis(alkylthio)-7,8-dicyanoquinodimethanes,[14,15] and 11,12-bis(alkylthio)-11,12-dicyano-2,6-naphthoquinodimethanes[16] was investigated in their solution polymerizations previously, and it was pointed out that the polymerization reactivity is exclusively determined by the steric effect of the alkoxy, acyl, and alkylthio substituents. Therefore, low reactivity of **2e** and **2f** with bulky alkoxy groups is due to the bulkiness of substituents, but the reason for low reactivity of **2a** and **2e**

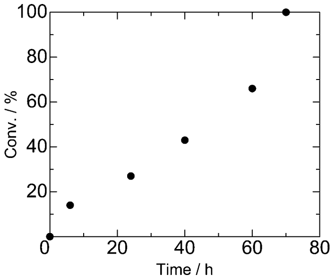

Figure 1. Time–conversion plot for photopolymerization of **2c** in the solid state.

with less bulky groups is not clear at present. It is plausible that the packing structure mode of the molecules in the crystals affects significantly the polymerization reactivity as pointed out previously for the solid-state polymerization of substituted quinodimethanes.[6]

The time–conversion plot for the photopolymerizations in the solid state of **2c** is shown in Figure 1, where the conversion increases with time and greatly at the latter stage.

Generally, time–conversion plots in solution and bulk polymerizations show convex curves because the polymerization rate becomes gradually slow at the latter stage for diminished monomer concentration. The time–conversion plot profile for the photopolymerization of **2c** in the solid state is significantly different from the conventional one in solution polymerization. The rise of the polymerization rate in the solid state might be due to the difference in the mobility of the molecules and the relative position of the molecules between the solid state and the solution. In the solution, collisions between monomer and monomer and between propagating polymer chain and monomer are diminished with a decrease in monomer concentration. On the other hand, in the solid state, the relative position of the monomer molecules does not change significantly compared with the solution because molecular movement is restricted, and moreover mechanical strain is imposed on the crystals upon polymerization.

Characterization of Polymer. The needlelike solids obtained by photopolymeriztion of **2c** in the solid state were characterized by ^{1}H and ^{13}C NMR and IR spectroscopies and powder XRD measurement. The ^{1}H NMR spectrum of polymer of **2c,** purified by dissolution–precipitation treatment, is shown in Figure 2, together with monomer **2c**.

The peaks at 8.59, 7.71, 6.63, and 6.56 ppm assigned to quinoid protons of monomer **2c** disappeared in the ^{1}H NMR spectrum of the resulting polymer, and new signals due to the phenylene protons were observed at 7.75 and 7.16 ppm. In the ^{13}C NMR spectrum, the peaks at 186.1 ppm due to the exocarbonyl carbon and 111.4 ppm due to the disubstituted exomethylene carbon of monomer **2c** disappeared, and new peaks at 155.8 ppm assigned to the carbon next to oxygen in the phenoxy group and at 64.4 ppm due to the quaternary carbon were observed. Also, a characteristic absorption band at 1504 cm^{-1} assigned to the exocyclic conjugated carbon–carbon double bond was absent in the IR spectrum of the resulting polymer. Those changes observed in the ^{1}H and ^{13}C NMR and IR spectra support that polymerization of **2c** takes place at the disubstituted exomethylene carbon atom and exocarbonyl oxygen with formation of the stable aromatic structure. The ^{1}H and ^{13}C NMR and IR spectra of polymer obtained by this solid-state polymerization were in good agreement with those of polymer obtained by the melt polymerization of **2c** in the presence of 2,2′-azobis(isobutyronitrile)(AIBN) as initiator, indicating that both polymers obtained by melt and solid-state polymerizations may have completely the same structure. Also, ^{1}H and ^{13}C NMR and IR spectra of polymers obtained by the photopolymerizations of other monomers **2b**, **2e**, **2d**, and **2f** were in good agreement with those of corresponding polymers obtained by the melt or solution polymerizations in the presence of AIBN.

Monomer crystals changed color from orange to pale yellow with retaining the crystal shape. Thus, we compared the monomer needle crystals with needlelike

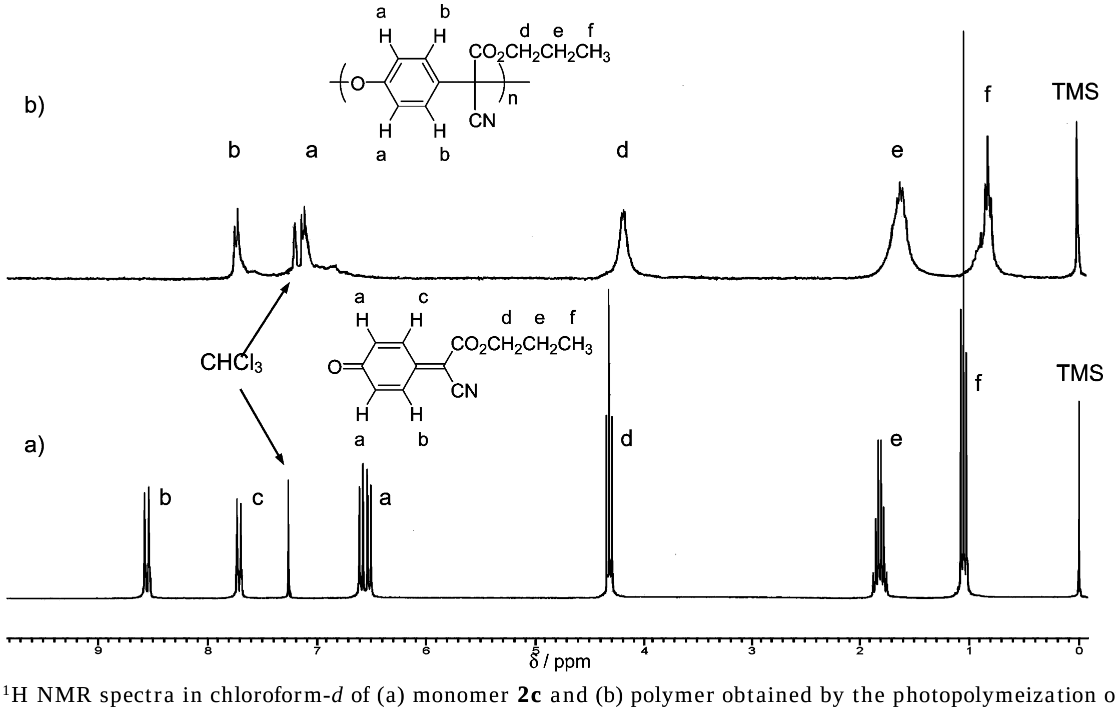

Figure 2. ^{1}H NMR spectra in chloroform-*d* of (a) monomer **2c** and (b) polymer obtained by the photopolymeization of **2c** in the solid state.

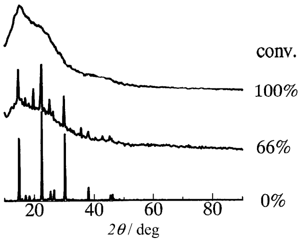

Figure 3. Powder XRD patterns of (a) monomer **2c**, (b) product at 66% conversion, and (c) product at 100% conversion obtained by the photopolymerization of **2c** in the solid state.

products in more detail by SEM measurement. The needlelike product obtained by photopolymerization in solid state has a smooth surface, and also the sharp edge observed in monomer crystals disappeared. This suggests strongly that the destruction of crystal lattice took place during polymerization.

To investigate crystallinity of polymers obtained, the powder XRD measurements at different conversions for the monomer **2c**, which showed the highest polymerization reactivity, were carried out. The powder XRD patterns of the monomer **2c** and the reaction mixtures at 66% conversion and at 100% conversion are shown in Figure 3.

The powder XRD pattern of the monomer **2c** showed very sharp peaks, but the powder XRD pattern at 100% conversion was broad, and there are no significant peaks, which implies that it is amorphous. The powder XRD patter at 66% conversion shows that both the monomer crystal phase and the polymer amorphous phase coexist. The remainder of this monomer crystal phase until relatively high conversion indicates that the polymerization takes place locally in the crystals; that is, polymerization starting at a defect in the crystal lattice or the crystal surface may proceed as heterogeneous reaction[1] where the chain growth will occur with a much higher probability around the preformed chain than elsewhere in the crystals.

Crystal Structure and Packing of Molecules. Previously, we discussed the relationship of the polymerization reactivity of the 7,7,8,8-(alkoxycarbonyl)quinodimethanes in the solid state with the molecular packing in the crystals on the basis of crystal structure analysis.[6] Here, we investigated the crystal structure of **2c** by X-ray crystallography to clarify the packing mode of the monomer molecules in the crystals. The single crystal of **2c** was prepared successfully by slow solvent evaporation from hexane/dichloromethane solution. The crystallographic data of **2c** are summarized in Table 3, and the crystal structure is shown in Figure 4 together with those of topochemically polymerizable **1a** (prism) for comparison.

2c molecules stack along one axis to form columnar structures as shown in Figure 5a. As defined previously, we investigated the stacking manners in the column

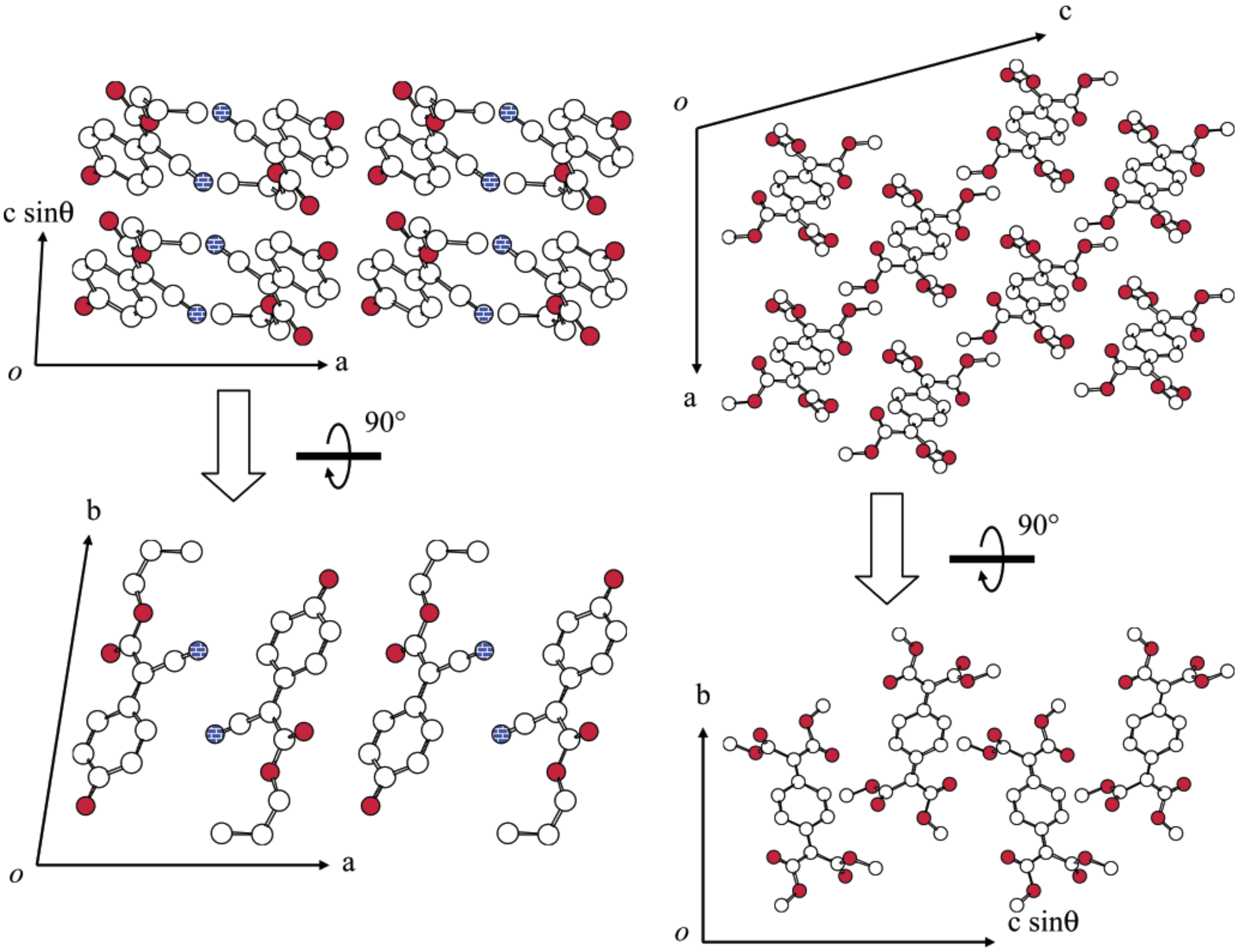

Figure 4. Crystal structures of monomers **2c** and **1a** (prism). Open and solid circles represent carbon and oxygen atoms, respectively. Hydrogen atoms are omitted for clarity.

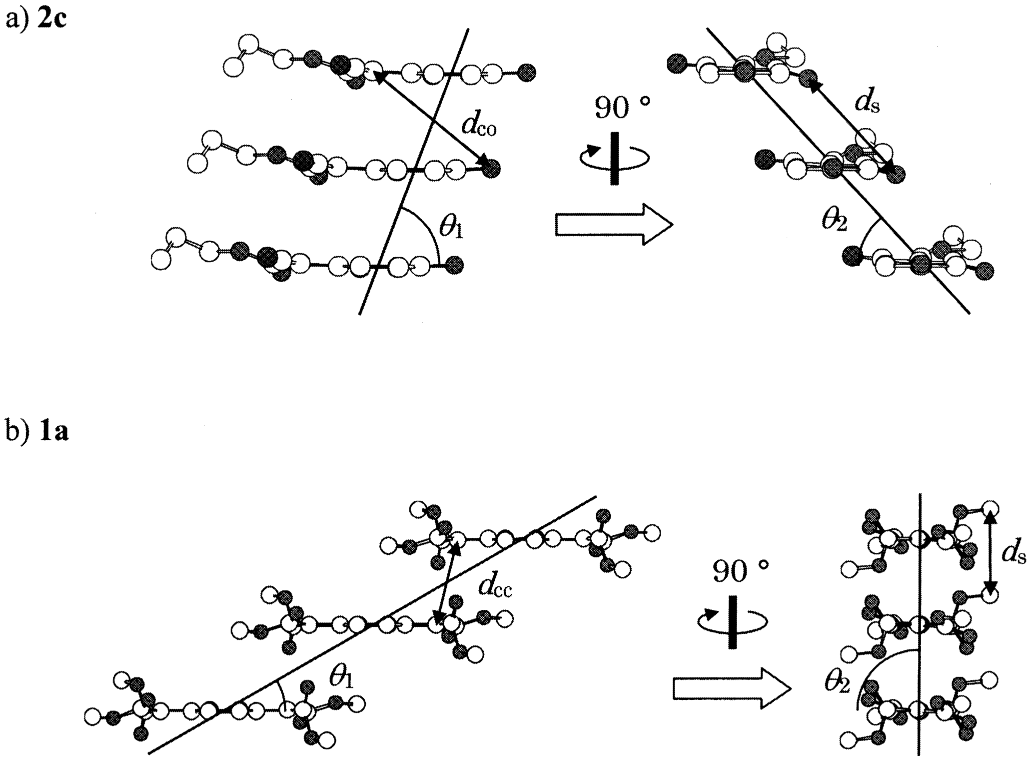

Figure 5. Stacking models for **2c** and **1a** (prism) in the crystals and the definition of stacking parameters for the prediction of the topochemical polymerization reactivity. d_s is the stacking distance between the adjacent monomers in a column; d_{co} and d_{cc} are the distance between the reacting exomethylene carbon and exocarbonyl oxygen or exomethylene carbon, respectively; θ_1 and θ_2 are the angles between the stacking axis and longer axis of the monomer molecule and the shorter axis of the molecule, respectively.

Table 3. Crystallographic Data for Crystal of 2c and 1a (Prism)

monomer	**2c**	**1a** (prism)
formula	$C_{12}H_{11}NO_3$	$C_{16}H_{16}O_8$
fw	217.22	336.29
crystal system	triclinic	monoclinic
space group	$P\bar{1}$ (#2)	$P2_1/n$ (#14)
a, Å	10.4163(5)	8.6787(7)
b, Å	11.914(1)	7.5719(7)
c, Å	4.7895(3)	12.761(1)
α, deg	91.125(2)	90
β, deg	92.977(3)	105.193(2)
γ, deg	80.613(1)	90
V, Å^3	585.59(7)	809.2(1)
Z	2	2
ρ_{calc}, g/cm^3	1.232	1.380
unique reflecns	1999	1828
no. of obsd reflecns	1996	1477
R_1	0.064	0.046
R, R_w	0.128, 0.154	0.106, 0.133
GOF	1.91	1.27
$2\theta_{max}$, deg	136.4	55.0
temp, °C	23	25

structure by using structural parameters (d_s, d_{co}, θ_1, and θ_2) to discuss molecular arrangements of monomers in the crystal structures in relation to the polymerization reactivity in the solid state of the substituted quinodimethanes.[6] In the case of **2c**, structural parameters of θ_1, θ_2, d_s, and d_{co} are to be 76°, 49°, 4.8 Å, and 6.3 Å, respectively. As a typical example of the topochemically polymerizable substituted quinodimethanes, the columnar structure of **1a** (prism) is shown in Figure 5b, where the corresponding parameters are to be $\theta_1 = 30°$, $\theta_2 = 89°$, $d_s = 7.6$ Å, and $d_{cc} = 3.9$ Å.[6] The structural parameters of **2c** are greatly different from those of **1a** (prism). It is considered, therefore, that this significant difference does not allow polymerization of **2c** in the solid-state photopolymerization to proceed topochemically, resulting in an amorphous polymer.

Conclusions

Thermal polymerizations and photopolymerizations of 7-alkoxycarbonyl-7-cyano-1,4-benzoquinone methides (**2a**–**f**) in the solid state were investigated. In the thermal polymerization in the solid state, **2a, 2c**, **2d**, and **2e** polymerized to give glassy solids or a mass of crystals, but both **2b** and **2f** did not polymerize. In the photopolymerization in the solid state, all monomer crystals except for **2a** polymerized to give corresponding polymers as needlelike solids, which were amorphous. Crystal structure of **2c** was determined by single-crystal X-ray structure analysis, and it was found that molecular packing of **2c** in the crystals is significantly different from that of topochemically polymerizable **1a** (prism). This difference resulted in the formation of amorphous polymer of **2c**.

Acknowledgment. A part of this work was supported by “Nanotechnology Support Project” of the Ministry of Education, Culture, Science and Technology (MEXT), Japan.

References and Notes

(1) Wegner, G. *Z. Naturforsch. B* **1969**, *24*, 824. (b) Wenger, G. *Pure Appl. Chem.* **1977**, *49*, 443. (c) Enkelmann, V. *Adv. Polym. Sci.* **1984**, *63*, 91. (d) Ogawa, T. *Prog. Polym. Sci.* **1995**, *20*, 943. (e) Huntsman, W. D. *The Chemistry of Functional Groups. Supplement C: The Chemistry of Triple-Bonded Functional Groups*; Patai, S., Rappoport, Z., Eds.; John Wiley & Sons: New York, 1983; Chapter 22. (f) Okada, S.; Matsuda, H.; Nakanishi, H. *Polymeric Materials Encyclopedia*; Salamone, J. C., Ed.; CRC Press: Boca Raton, FL, 1996; p 8393. (g) Bloor, D.; Chance, R. R. *Polydiacetylenes*;

NATO ASI Series E, Applied Sciences No. 102; Martinus Nijhoff: Dorddrecht, 1985.
(2) Hasegawa, M. *Chem. Rev.* **1983**, *83*, 507. (b) Hasegawa, M. *Adv. Phys. Org. Chem.* **1995**, *30*, 117.
(3) Kiji, J.; Kaiser, J.; Wegner, J. G.; Schulz, R. C. *Polymer* **1973**, *14*, 433. (b) Enkelmann, V. *Chem. Mater.* **1994**, *6*, 1337. (c) Xiao, J.; Yang, M.; Lauher, J. W.; Fowler, F. W. *Angew. Chem., Int. Ed.* **2000**, *39*, 2132. (d) Hoang, T.; Lauher, J. W.; Fowler, F. W. *J. Am. Chem. Soc.* **2002**, *124*, 10656.
(4) Matsumoto, A.; Matsumura, T.; Aoki, S. *Macromolecules* **1996**, *29*, 423. (b) Matsumoto, A.; Yokoi, K.; Aoki, S.; Tashiro, K.; Kamae, T.; Kobayashi, M. *Macromolecules* **1998**, *31*, 2129. (c) Matsumoto, A.; Odani, T.; Chikada, M.; Sada, K.; Miyata, M. *J. Am. Chem. Soc.* **1999**, *121*, 11122. (d) Matsumoto, A.; Nagahama, S.; Odani, T. *J. Am. Chem. Soc.* **2000**, *122*, 9109. (e) Odani, T.; Matsumoto, A. *Macromol. Rapid Commun.* **2000**, *21*, 40. (f) Matsumoto, A.; Katayama, K.; Odani, T.; Oka, K.; Tashiro, K.; Saragai, S.; Nakamoto, S. *Macromolecules* **2000**, *33*, 7786. (g) Nagahama, S.; Matsumoto, A. *J. Am. Chem. Soc.* **2001**, *123*, 12176. (h) Matsumoto, A.; Odani, T. *Macromol. Rapid Commun.* **2001**, *22*, 1195. (i) Matsumoto, A.; Sada, K.; Tashiro, K.; Miyata, M.; Tsubouchi, T.; Tanaka, T.; Odani, T.; Nagahama, S.; Tanaka, T.; Inoue, K.; Saragai, S.; Nakamoto, S. *Angew. Chem., Int. Ed.* **2002**, *41*, 2502. (j) Matsumoto, A.; Tanaka, T.; Tsubouchi, T.; Tashiro, K.; Saragai, S.; Nakamoto, S. *J. Am. Chem. Soc.* **2002**, *124*, 8891. (k) Tanaka, T.; Matsumoto, A. *J. Am. Chem. Soc.* **2002**, *124*, 9676.
(5) Itoh, T.; Nomura, S.; Uno, T.; Kubo, M.; Sada, K.; Miyata, M. *Angew. Chem., Int. Ed.* **2002**, *41*, 4306.
(6) Nomura, S.; Itoh, T.; Nakasho, H.; Uno, T.; Kubo, M.; Sada, K.; Inoue, K.; Miyata, M. *J. Am. Chem. Soc.* **2004**, *126*, 2035.
(7) Iwatsuki, S.; Itoh, T.; Meng, X. *Macromolecules* **1993**, *26*, 1213.
(8) Itoh, T.; Fujinami, H.; Yamahata, M.; Konishi, H.; Kubo, M. *Macromolecules* **1998**, *31*, 1501.
(9) Itoh, T.; Wanibe, T.; Iwatsuki, S. *J. Polym. Sci., Part A: Polym. Chem.* **1996**, *34*, 963.
(10) Itoh, T.; Iwatsuki, S. *Macromol. Chem. Phys.* **1997**, *198*, 1997.
(11) Iwatsuki, S.; Itoh, T.; Sato, T.; Higuchi, T. *Macromolecules* **1987**, *20*, 2651.
(12) Iwatsuki, S.; Itoh, T.; Higuchi, T.; Enomoto, K. *Macromolecules* **1988**, *21*, 1571.
(13) Iwatsuki, S.; Itoh, T.; Yabunouchi, H.; Kubo, M. *Macromolecules* **1990**, *23*, 3450.
(14) Iwatsuki, S.; Itoh, T.; Sato, T.; Miyashita, I. *Macromolecules* **1988**, *21*, 557.
(15) Iwatsuki, S.; Itoh, T.; Sato, T.; Kusaka, N.; Maeno, H. *Macromolecules* **1992**, *25*, 6395.
(16) Itoh, T.; Ario, T.; Kido, M.; Iwatsuki, S. *Macromolecules* **1994**, *27*, 7035.

MA049596R